Applied Physics Reviews

REVIEW ARTICLE | MAY 30 2024

Virus inactivation by matching the vibrational resonance

Mohammad Sadraeian ; Irina Kabakova ; Jiajia Zhou ; Dayong Jin

Appl. Phys. Rev. 11, 021324 (2024)
https://doi.org/10.1063/5.0183276

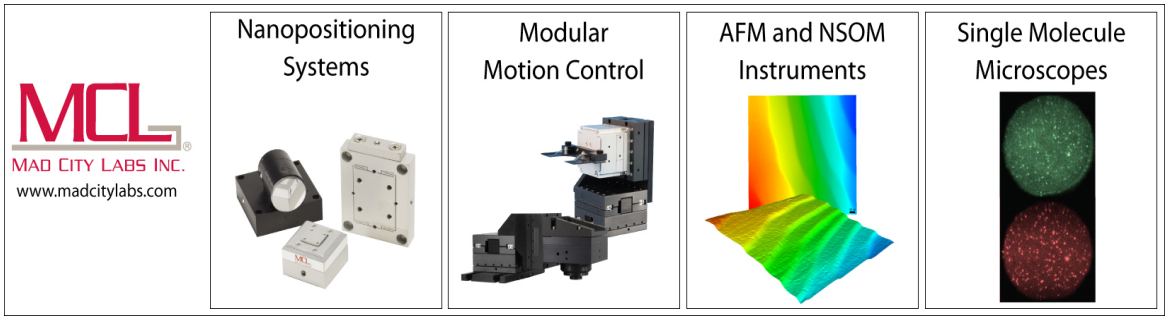

AIP Publishing

Applied Physics Reviews REVIEW pubs.aip.org/aip/are

Virus inactivation by matching the vibrational resonance

Cite as: Appl. Phys. Rev. **11**, 021324 (2024); doi: 10.1063/5.0183276
Submitted: 22 October 2023 · Accepted: 26 April 2024 ·
Published Online: 30 May 2024

Mohammad Sadraeian,[1,2] Irina Kabakova,[1,2] Jiajia Zhou,[1,2,a)] and Dayong Jin[1,2,a)]

AFFILIATIONS

[1]Institute for Biomedical Materials and Devices (IBMD), Faculty of Science, University of Technology Sydney, Sydney, NSW 2007, Australia
[2]ARC Centre of Excellence in Quantum Biotechnology (QUBIC), Institute for Biomedical Materials and Devices (IBMD), Faculty of Science, University of Technology Sydney, Sydney, NSW 2007, Australia

[a)]**Authors to whom correspondence should be addressed:** jiajia.zhou@uts.edu.au. **Tel.:** +61426574596 and dayong.jin@uts.edu.au. **Tel.:** +61433875470

ABSTRACT

Physical approaches based on irradiation provide advances for the prevention and treatment of viral infections, while recognizing that certain chemical inactivation techniques demonstrate significant effectiveness alongside physical methods. By generating resonant vibrations of complete virus particles, which are in the GHz range and quite high compared to that of human cells, viruses can be inactivated. Therefore, exposure to ultrasound waves or non-thermal microwaves with a suitable resonant frequency oscillating electric field holds the potential to neutralize the virus particle with no damage to human. The deactivation mechanism could be a result of the mechanical effect or oxidation stress, and in this article, we discuss the elucidation of these effects on the virus' structure. We also explore the current state and future prospects of the anti-viral methods based on acoustic cavitation via ultrasound and non-thermal microwave, addressing critical needs in virology.

TABLE OF CONTENTS

I. INTRODUCTION

The recent outbreaks of respiratory viruses, such as various types of influenza viruses[1] and coronaviruses,[2] have highlighted the difficulties in controlling virus transmission and inactivation. Virus transmission in the environment depends on the ability of viral particles to remain infectious. Viral morphology showcases a diverse array of shapes, from filamentous and icosahedral structures to enveloped forms with outer membranes and bacteriophages with distinctive head and tail configurations. Beside the shape, human viruses exhibit varied structures, with enveloped viruses like HIV and SARS-CoV-2 featuring an outer lipid bilayer envelope containing glycoproteins that facilitate binding to host cell receptors. In contrast, non-enveloped viruses, lacking this lipid envelope, present a more resilient nucleocapsid structure.[3] Enveloped viruses, such as HIV and SARS-CoV-2, can specifically bind to the host cell receptors through Env glycoprotein[4] and spike,[5,6] respectively. Antiviral drugs and active molecules are capable of inactivating virion to prevent the cell attachment,[7,8] whereas these chemical drugs have major limitations. Viruses can resist inactivation by chemical drugs due to their small size, lack of cellular structure, rapid mutations, and explicit propagation.[9,10] In order to prevent

drug resistance and their side effects, scientists have introduced physical methods based on irradiation to disrupt viral functions.[11]

The viral inactivation through irradiation strategies are preferred to have non-thermal effect and being non-destructive to our body. The use of ionizing radiation, especially ultraviolet, x-ray, and gamma rays, despite the high ability to inactivate viruses, can cause damage to human cells, as discussed elsewhere.[12] Combination of the irradiation-dependent tools with sensitizers, which is called a photodynamic therapy (PDT)—a technique that involves the use of light-activated chemical sensitizers to inactivate viruses, is considered efficient in virus inactivation. However, PDT remains subject to several limitations and side effects, due to the presence of a chemical sensitizer and obstacles in its activation in deep tissue by light, as discussed elsewhere.[13] The application of ultrasound (also known as acoustic cavitation) and non-thermal microwave may overcome the limitations of irradiation-based viral inactivation, provided that the mechanical resonance vibration of the virus can be precisely targeted and harnessed for effective viral disruption [Fig. 1(a)].[14,15]

The use of ultrasound waves for virus inactivation involves two main types of cavitation, transient (inertial) and stable (non-inertial), schematically shown in Figs. 1(b) and 1(c), respectively. These two types are distinguished by the size of a bubble and consequently the level of pressure they generate. Formation of bubbles can be achieved by using an ultrasound transducer, as depicted in Fig. 2(a). Both stable and inertial cavitation produce mechanical forces, with inertial cavitation also leading to the formation of a hotspot with extreme pressure and/or temperature where chemical effects are possible [Fig. 2(b)]. These effects, whether sonomechanical [independent of reactive oxygen species (ROS)] or sonochemical (sonoluminescence and sonochemistry) [Figs. 2(c) and 2(d)], contribute to the inactivation of viruses.

Unlike ultrasound waves that are mechanical waves,[16,17] the microwaves are electromagnetic wave radiation.[18] By using non-ionizing microwaves within dosage safety standards[19,20] that match the vibrational resonance frequency of the virus, such as SARS-CoV-2, the electromagnetic radiation can penetrate the human body without causing harm,[21,22] leading to virus inactivation. This technique could be applied using a waveguide [Fig. 2(e)] generating microwaves. This inactivation can occur through two mechanisms: via resonant vibrations of individual spikes and collapse of the entire shell. The spike protein trimer, thermostable in its closed conformation,[23] becomes vulnerable under weak and moderate electric fields[24,25] due to mechanical changes, such as bowing toward the virion membrane and breaking[25] [Fig. 2(f)]. Leveraging this effect, electromagnetic denaturation of the spike has been demonstrated using temperature-controlled microwave exposure.[26] Further studies show targeted virus inactivation through mechanically altering the spike proteins' specific vibrational signature inherent in the virus ensemble.[27]

Beside the spike, the core–shell of virion being a potential target for this type of inactivation. Microwaves with the frequency matched to the acoustic vibrations inside spherical virions and consequently resonate through a process called microwave resonant absorption (MRA).[28] The resonance is influenced by the virus's intrinsic factors, such as hydration level, surface charge, surrounding media, and size. In this review, we will highlight the importance of further investigating these factors to optimize viral inactivation [Fig. 2(g)].

Both of ultrasound and microwaves share similar characteristics, which make them potential tools for virus inactivation, including

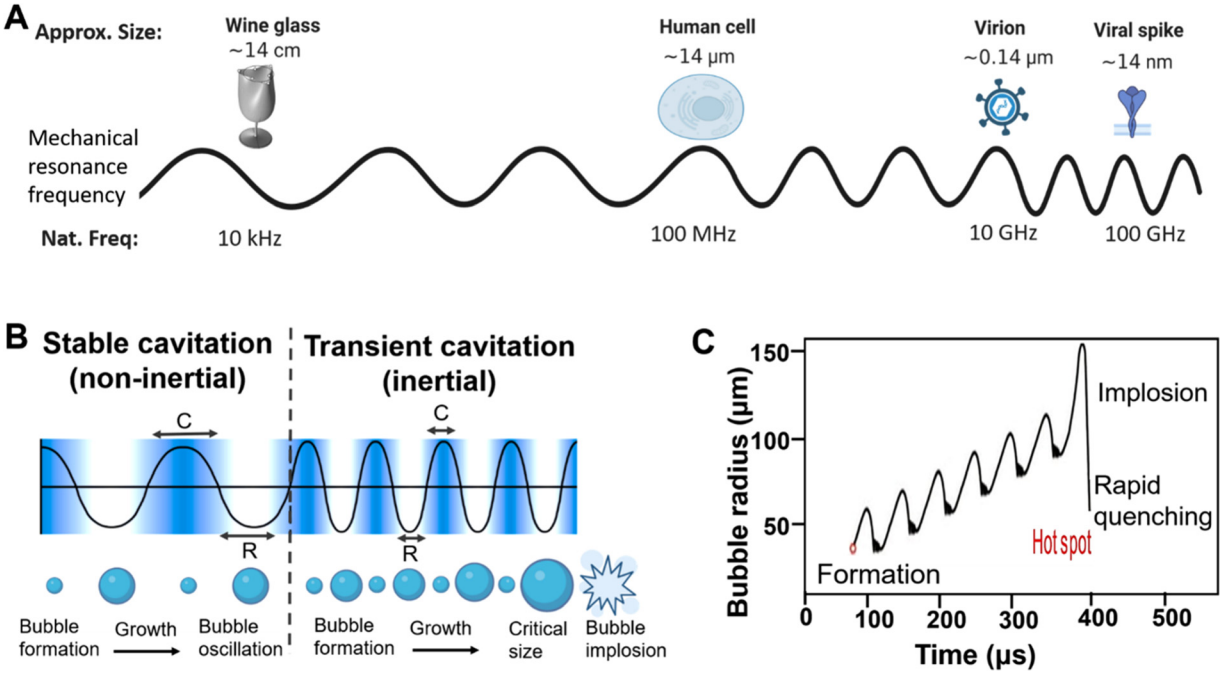

FIG. 1. (a) A frequency scale of mechanical vibrations with representative dimensions of viruses being in hundreds of nanometers and their frequencies of tens of GHz, which is quite high compared to human cells with frequencies of tens of MHz. (b) Schematic explanation of cavitation mechanism: R and C are regions of rarefaction and compression. (c) In transient cavitation, bubbles grow until they become unstable and implode causing rapid quenching and killing of viruses within the bubble.

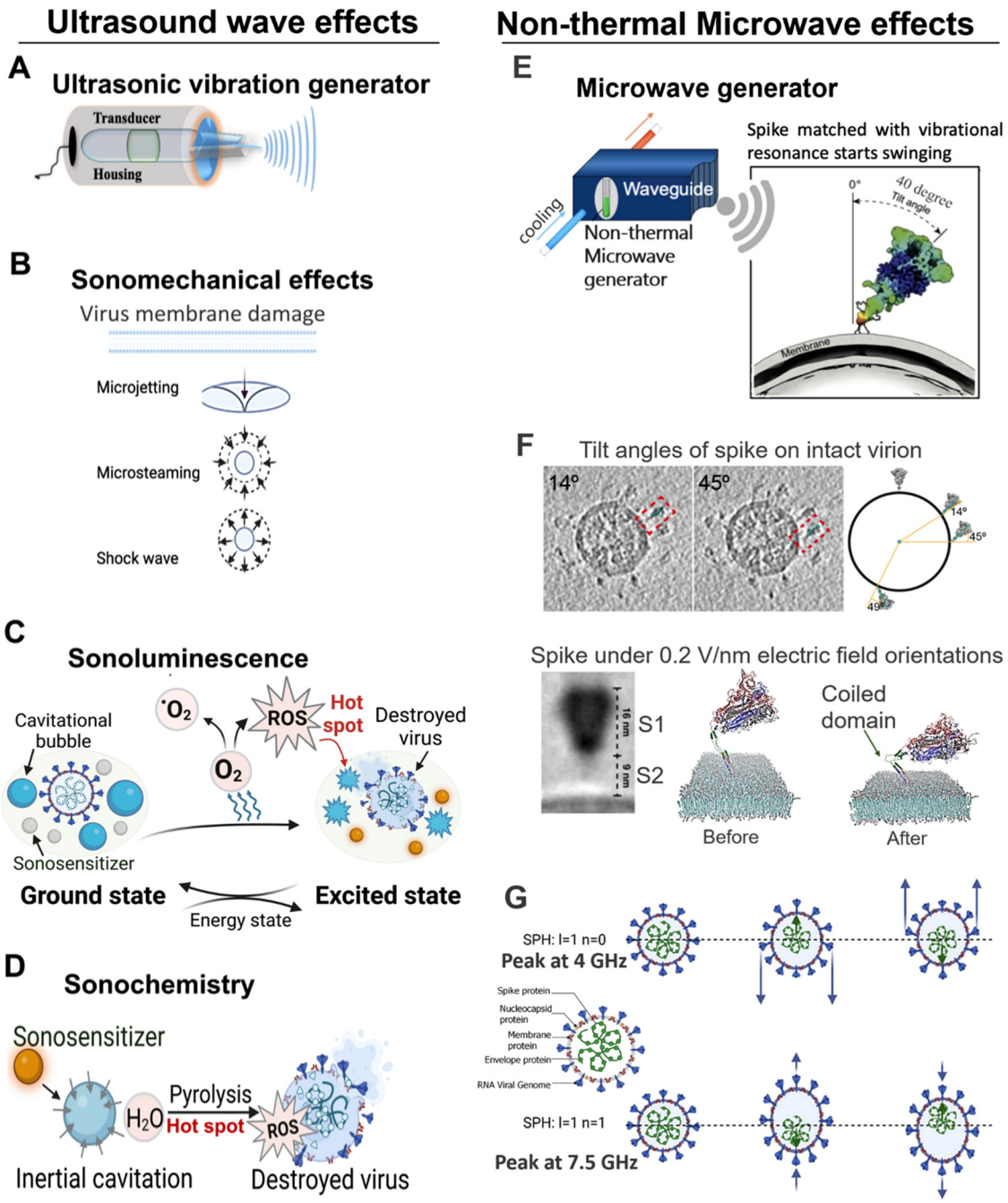

FIG. 2. Effects of ultrasound (a)–(d) and microwaves (e)–(g) on virus: (a) Schematic picture of an experimental apparatus for ultrasonic vibration. Possible effects of acoustic cavitation on virus include, sonomechanical (b) and sonochemical (sonoluminescence, sonochemistry) (c) and (d) effects.[30] Created with BioRender.com. (e) Schematic picture of a microwave waveguide and its connection to an efficient cooling system. Reproduced with permission from Afaghi *et al.* Sci. Rep. **11**, 23373 (2021). Copyright 2021 Authors, licensed under a Creative Commons Attribution (CC BY) license.[26] (f) In the upper panel, TEM images and scheme demonstrate spike tilt angles (14°, 45°, and 49°) toward the membrane for the intact virion. Reproduced with permission from Ke *et al.*, Nature **588**, 498–502 (2020). Copyright 2020 Springer Nature.[31] The lower panel demonstrates the S1 and S2 subunits at 16 and 9 nm in length, respectively. Molecular dynamics simulations reveal that applying a 0.2 V/nm electric field (EF) perpendicular to the spike leads to the denaturation of the S2 subunit,[25] corroborating earlier simulation under weak EF[24] and experimental findings on spike protein denaturation through temperature-controlled microwave exposure.[26] Reproduced with permission from Kuang *et al.* Sci. Rep. **12**, 12986 (2022). Copyright 2022 Authors, licensed under a Creative Commons Attribution (CC BY) license.[25] (g) Schematic illustrating the displacement of two dipolar modes of the spherical (SPH) virion, with angular momentum $l = 1$ and with quantum numbers $n = 0$ or 1, representing the peaks at 4 and 7.5 GHz of microwave, respectively. Reproduced with permission from Wang *et al.* Sci. Rep. **12**, 12596 (2022). Copyright 2022 Authors, licensed under a Creative Commons Attribution (CC BY) license.[32]

acoustic vibration of molecules, resonance in virus structure, high penetration ability, and plasma release.[17,29] In this review, we summarize the nonthermal effects of microwaves, radio-waves and ultrasound on virus structure, and introduce the anti-viral application of these waves. Moreover, we discuss the factors affecting the efficiency of inactivation, such as the physical properties of both wave and targeted virus, as well as its surrounding media, including water, air, and surfaces, to prevent virus spread, while paving the way for future studies on virus–cell interactions to potentially halt virus propagation in infected tissues (Table I).

II. ULTRASOUND WAVES

A. Types of cavitation and their effects on virus

For decades, ultrasound has been used for disease diagnosis[41] and therapy.[42,43] Due to the safety and relatively noninvasive nature of ultrasound, it has been applied for cell membrane permeabilization and sonoporation. According to multiple studies, the ultrasound can be employed for microbial inactivation.[44–46] As an instance, the use of ultrasound instead of destructive irradiation methods may overcome the limitations of antimicrobial photodynamic inactivation (aPDI) in deep tissue.[13] This combination is called sono-photodynamic therapy (SPDT) with promising approaches toward viral disinfection, although some challenge in selective harmless inactivation remain.[15]

Ultrasound is a general name of ultrasonic cavitation or Acoustic cavitation (AC). Ultrasound-induced cavitation generates bubbles whose collapse significantly increases temperature and pressure at their center.[47,48] Focused ultrasound delivered externally can mechanically destroys tissue through acoustic cavitation.[49,50] This ablation technique is called boiling histotripsy,[51] has demonstrated promising results in preclinical and clinical studies,[49,52] but concerns remain about tumor metastasis, warranting further investigations. Ultrasound treatment

TABLE I. A list of virus inactivation studies using cavitation resonance techniques.

Techniques	Radiation detail	Virus species	Media	Inactivation rate detail	Reference
Ultrasound (acoustic cavitation)	Ultrasound, frequencies (582, 862, and 1142 kHz), 120 min	Bacteriophages ΦX174 and MS2	Water	Inactivation rate coefficient (λ): 0.193 min^{-1} at 582 kHz (MS2) and 0.055 min^{-1} at 582 kHz (ΦX174)	33
	Ultrasound, Frequencies (28 kHz), 600W, 120 min	Phytoviruses ACLSV in plum and apricot. TMV in tomato	Fruits (plum and apricot)	87.5% inactivation of ACLSV, and 80.5% inactivation of TMV	34
	Solo ultrasound without sonosensitizer, frequencies (1.8 MHz), 2.16 W/cm^2, 5 min	Enveloped virus (parainfluenza HPIV3) and non-enveloped Enterovirus D68 (EV-D68)	Water	HPIV3 titer ($Log_{10}TCID_{50}$/ml) reduced by about 10^4 times within 5 min, while EV-D68 achieved a similar reduction by 10^4 times after 10 min	35
	Ultrasound, 27 and 42 kHz at a power density of 1.60 W/cm^2 at 300 min under CO_2-shielding gas	Surrogate models of HCV, Herpes virus and Parvovirus B19	Blood plasma	Virus titer in plasma ($Log_{10}TCID_{50}$/ml): 2.5 (BVDV), 4.6(SFV), 3.4 (PRV), 0 (PPV)	36
Non-thermal microwaves	Radiofrequency, super-high frequency (SHF) 10–17 GHz	Clinical SARS-CoV-2, COVID-19 patient-specific exposure	Human body	100% inactivation using 14.5 ± 1 W/m^2 patient–specific exposure duration of 15 min	22
	Microwave, 8–8.4 GHz	Influenza A virus (H3N2)	Water	38% inactivation using 87 V/m (82 W/m^2). 100% inactivation using 273 V/m (810 W/m^2)	37
	Microwave, 7 GHz	Bovine coronavirus (BCoV)	Water	880 W/m^2, 53.9% inactivation (<3 log)	27
	Microwave, 15.0–19.5 GHz	Human coronavirus (HCoV-229E)	Culture medium	2 Watts, Waveguide size WR-62, 7.5 min, 3-log inactivation	38
	Microwave, 700 W, 10 GHz	SARS-CoV-2	Aerosol	400 V/m, 65.9% inactivation	39
	Microwave, 700 W, 2.45 GHz	SARS-CoV-2	Deionized water	2 min; spike denaturation ~95%	26
	Microwave, 2.8 and 5.6 GHz	Bovine coronavirus (BCoV)	Dry surface	6.1–6.5 W/m^2, insignificant inactivation less than 90%	40

offers a promising method for virus inactivation in fluids like blood plasma, demonstrating minimal impact on coagulation proteins and no cytotoxic effects.[36] The cavitation phenomenon, induced by low-intensity ultrasound in aqueous environment, involves bubble oscillations without significant size change, driven by acoustic pressure.[30,53]

Based on the degree of extreme pressure or temperature, the cavitation process is categorized into transient (inertial) or stable (non-inertial), resulted from higher and lower acoustic pressures, respectively [Fig. 2(a)]. Stable cavitation generates mechanical effects through oscillatory bubble dynamics, affecting nearby entities like cells. In contrast, transient cavitation involves more vigorous bubble activity due to surrounding liquid dynamics, potentially disrupting adjacent structures.[30] Inertial cavitation involves bubbles undergoing rapid contraction and collapse, concentrating and then releasing substantial energy into the focal area. The entire process of inertial cavitation occurs within approximately 400 μs. This phenomenon generates energy leading to the formation of localized hot spots characterized by extremely high temperatures (around 5000 K) and pressures (about 250 MPa), creating extreme conditions that induce mechanical, thermal, and chemical effects.[47] Both stable and inertial cavitation can exert mechanical forces, along with chemical effects initiated by inertial cavitation. Regardless of the type of cavitation, whether sonomechanical (ROS-independent) or sonochemical (sonoluminescence, sonochemistry), it can contribute to the inactivation of viruses [Figs. 2(b)–2(d)].[54]

The exact mechanism by which cavitation works on the vibration and inactivation of viral particle has not yet been elucidated, and a clear mechanism has not yet established such an effect.[48,55,56] Herein, we discuss three potential mechanisms through which cavitation impacts viruses, including chemical effects, thermal effects, and mechanical vibration. The formation and collapse of bubbles within the liquid medium can generate pressure shocks reaching several 100 MPa. Unsymmetrical collapse of bubbles may form microjets with velocities exceeding 100 m/s. These theoretical aspects of acoustic cavitation are discussed by Yusof *et al.*[48,57] The subsequent mechanical effects, such as liquid microjets, highly localized shear forces, and microstreams, can physically destroy, weaken, or rupture the outer membrane of any type of microorganism.[58] In addition, these mechanical effects accompanied by acoustic streaming effect generated by bubble collapses can enhance mass transfer, thereby boosting the rate constants of chemical reactions.[48,57]

In addition, the intense temperatures, reaching several 1000 K estimated at the center of collapsing bubble (so-called hotspot), lead to the formation of highly reactive redox radicals, which can initiate various chemical reactions.[48] In addition to the chemical effect, the extreme temperatures can locally damage microorganisms or at least compromise the integrity of their outer membrane and make them more susceptible to further damage caused by reactive species.[59]

Acoustic cavitation emerges as a promising technique for the inactivation of water-mediated viruses, targeting pathogens that impact both human health, such as Enteroviruses including poliovirus, and agriculture, like Potato virus Y (PVY). However, the application of acoustic cavitation to waterborne viruses encounters significant limitations: (1) larger volumes of water cannot be treated continuously; batch operations are the only option, (2) operating piezo transducers for a prolonged period of time consumes a tremendous amount of energy, and (3) it is difficult reaching to an industrial scale.

Acoustic cavitation (AC), distinguished by its resonance-based technique for virus inactivation through ultrasonic wave-induced bubble generation, contrasts with hydrodynamic cavitation (HC) which relies on fluid dynamics without resonance. HC occurs as liquid flows past an obstruction or through a constricted path, decreasing pressure to below the vaporization threshold and forming cavitation bubbles, useful for antimicrobial applications, such as in irrigation water treatments.[56] Similar to acoustic cavitation, HC induces physical and chemical changes due to the mechanical effects and ROS generation, respectively. Both chemical and mechanical effects can lead to changes in the structure of pathogens, such as virus, which makes the cavitation an applicable tool for water disinfection.[56] This anti-viral application is described in the next sections (see Secs. II B–II D). There are limited reports on the cavitation for anti-viral purposes[33,36,60] using HC against MS2 bacteriophage,[61] PVY plant virus,[62] as non-enveloped viruses, and Phi6 enveloped virus,[63] as a SARS-CoV-2 surrogate.

These studies delineate how HC disrupts the viral structure, setting it apart from acoustic cavitation's inactivation approach. Initial studies, such as Kosel *et al.*'s demonstrated a 4-log reduction in MS2.[61] Further investigation by Filipić *et al.*[62] into HC's ability to deactivate the PVY virus underlines the potential of mechanical stress over chemical effects in virus deactivation, emphasizing HC's distinct mechanism from AC in targeting waterborne viruses. The research by Zupanc *et al.*[63] on HC inactivating Phi6 further underscores this, demonstrating that mechanical effects are crucial for inactivation, particularly at lower temperatures, with increased temperatures enhancing susceptibility. The disruption of the lipid bilayer, rather than genome damage, was pinpointed as the primary inactivation mechanism.

B. Chemical effects of cavitation on virus composition

Virus inactivation by ultrasound is contingent upon various factors, such as ultrasonic power, wave amplitude, sample volume, temperature, composition, and the specific attributes of the virus, including its shape, size, and composition.[64] Viruses range in size from 20 to 300 nm, much smaller than prokaryotic cells. Viruses are broadly categorized by their composition; non-enveloped viruses consist of nucleic acid (either DNA or RNA) encased by a protein capsid, while enveloped viruses also include an outer lipid bilayer that encloses the capsid. The schematic structure of SARS-CoV-2, as an enveloped RNA virus is depicted in Fig. 2(g). Viral envelopes can also contain proteins and fatty acids. Most viruses are composed of a highly symmetric structure; icosahedral and helical symmetry are the two most common.[3] As a result of structural diversity, viruses have different levels of resistance to physico-chemical treatments.

It is possible for viruses to resist the chemical effects of cavitation at different pressure resistance levels.[65] As discussed above, the ultrasonic irradiation is associated with chemical effects related to the generation of destructive oxidants (H· and OH·) through the implosion of cavitation microbubbles.[57] These reactive species can oxidize important constituents of virus structure, protein capsid, lipoprotein envelope, genome, and glycoproteins on the surface.[66] The hydroxyl free radical (OH·) are potent oxidants known for their reactivity, readily oxidizing various species they come across or forming hydrogen peroxide (H_2O_2) as a result of self-reaction. Consequently, the free radicals produced during cavitation, coupled with mechanical effects, may contribute to virus inactivation by oxidizing the protein capsid and genome,[62] albeit to varying extents based on the structure of the virion.

The virus capsid composition might affect the time of inactivation. Chrysikopoulos *et al.*[33] showed the inactivation of ΦX174

(with hydrophilic capsid) was relatively slower than MS2 (with hydrophobic capsid) under the same treatment conditions. This suggests that ultrasound-induced cavitation, by generating reactive oxygen species such as hydroxyl radicals, not only damages viral components but also specifically targets the capsid's integrity and its surface recognition sites, thereby facilitating virus inactivation.

The virus envelopes are composed mainly of membrane proteins (M), envelope proteins (E), and spike proteins (S).[3] Lipids originate entirely from the host cell and vary based on the site of virus budding through the cellular membrane, whereas the envelope glycoproteins are encoded by the virus itself. Lipid peroxidation occurs when OH· attacks unsaturated fatty acids in lipids, resulting in chain reactions that generate other ROS.[67] There are several studies dealing with effects of free radicals and H_2O_2 on the lipoprotein membrane of bacteria and yeast,[67,68] not on viruses, although some studies compare lipidated viruses to non-lipidated ones.[36] By the breakage of the glycoside backbone, the free radicals can fragment the bio-polymer, thus changing its functionality. Additionally, sulfated polysaccharides are more susceptible to radical attack because of their composition.[69]

C. Mechanical effects of cavitation for virus inactivation

Ultrasound, through mechanical effects of cavitation, can either inactivate viruses by damaging their membranes[33] with intense pressure and heat or, conversely, facilitate virus entry into cells by mechanically permeabilizing the cell membrane,[70,71] especially when paired with microbubbles. This dual application hinges on controlling ultrasound parameters—like power intensity, frequency, and exposure time—to either destroy viruses or aid in virus transduction, thereby leveraging ultrasound potential by finely balancing its destructive and permeabilizing capabilities for targeted medical or industrial interventions.[72]

The effect of ultrasound on the permeabilization of the cell membrane for oncolytic HSV-1 entry was evaluated.[71] Vero monkey kidney cells infected with HSV-1 were exposed to 1 MHz ultrasound for a specified duration. The number of viral plaques in the ultrasound-treated cells was significantly higher than untreated control.[73] Plaque numbers were further increased by combining ultrasound with microbubbles. Similar outcomes were observed with another type of HSV-1 and oral squamous cell carcinoma (SCC) cells. Optimal plaque enhancement was achieved with ultrasound parameters of 0.5 W/cm^2 intensity, 20% duty cycle, and 10 s duration. However, cell viability was reduced by micro-bubble ultrasound at an intensity of 2.0 W/cm^2, at 50% duty cycle, or for 40 s. Using ultrasound promotes HSV-1 entry into cells, which make the ultrasound an useful tool to enhance the effectiveness of HSV-1 infection in oncolytic virotherapy.[71]

Through computer modellings, it was possible to model how the virus responded to mechanical vibrations over a wide range of ultrasound frequencies. Results showed that vibration between 25 and 910 MHz caused the virus shell to collapse and rupture within microseconds (0.35 μs at 110 MHz, 0.13 μs at 50 MHz, and 0.1 μs at 25 MHz). Additionally, resonant vibration of spikes throughout the shell occurred at 107 MHz. Furthermore, the resonant frequencies of the spike-free shell in the bouncing mode were 340 MHz, but this decreased to 312 MHz in the presence of spikes. Figure 3(a) demonstrates the effect of ultrasound vibration mode on the elastic properties of spikes and shells.[74] While discussing mechanical effects, it is pertinent to note that cavitation can indirectly lead to radical formation, which may complement mechanical stresses in damaging viral structures.[72]

Harmonic mechanical vibration from ultrasound waves, even below the lowest resonant modes, could induce significant vibration amplitudes in spikes. Within a fraction of a millisecond, spikes could experience high maximum principal strain values.[74] For enveloped viruses, it is possible to inactivate viruses through two mechanisms: transient vibrations of the lipid membrane alongside resonant vibrations of individual spikes and the buckling or collapse of the entire shell.[75] In contrast, non-enveloped viruses, such as EV-D68, show higher resistance to such treatment,[35] indicating a variance in ultrasound's effectiveness based on viral structure. This suggests that while ultrasound can inactivate enveloped viruses by targeting their lipid membranes and protein spikes, non-enveloped viruses may require different strategies for inactivation due to their more resilient capsid structures.[35] Both mechanisms suggest ultrasound's potential to mechanically inactivate viruses through structural compromise, showcasing its versatility in targeting different viral architectures.

The spike proteins of SARS-CoV-2 are usually geometrically different, and each spike protein has a different frequency with little difference. Yao and Wang designed an ultrasonic vibration exciter to inactivate the virus from infected human cells.[75] The frequency range was set as the first-order bending vibration frequencies 1.9×10^8–2.0×10^8 Hz with 360° rotating sweep excitation to human body, and the amplitude larger than 1.041×10^{-5} to ensure resonance excitation of every viral spike. Remarkably, this lumped parameter mechanical model effectively and safely can inactivate the SARS-CoV-2 virus.

Computational studies on the variants of the SARS-CoV-2 have revealed that the vibration modes of spike swing are constantly the lowest order which occupy up to about 50 orders of the vibration shapes of the virus with 25 spikes. The ultrasound wave of single frequency ω_e results in vibration and swing on the root of spike with 45° tilt angle.[76] Previously, TEM microscopic measurements have revealed that the spike tilt angles of 14°, 45°, and 49° toward the membrane for the intact virion[31,77] [Fig. 2(f)]. The ultrasound wave of single frequency ω_e results in vibration and swing on the root of spike.[76] Hence, acute spike swing could be resonantly stimulated by ultrasonic wave with intensity lower than 15 kPa to break the viral spike. The natural frequencies associated with spike swing basically fall into the ranges of (0.07 GHz, 0.12 GHz) or (0.26 GHz, 0.44 GHz) considering the potential increase in temperature [Fig. 3(b)].[76] By covering these ranges of natural frequencies of spike swing, the ultrasound wave can resonantly break the viral spikes in less than 180 ns (t = 159ns). Therefore, this simulation validates two frequency scanning strategies for SARS-CoV-2 inactivation using ultrasonic waves, targeting the virion's natural frequencies. The first strategy involves continuously adjusting the frequency ratio (ω_e/ω_0) from 0.5 to 2.0, enabling a dynamic match with the virus's resonance. The second employs a stepwise frequency change across four intervals, allowing for precise targeting of the viral spike's natural frequencies. The variants of SARS-CoV-2 show similar spike vibration shape, accompanied by which the corresponding natural frequency fall into some certain range.[48,76] Thus, this strategy could be utilized analogously to inactivate variants of coronavirus, extendable to the other viruses.

Studying the mechanism of mechanical effects as a singular effector on virus inactivation presents challenges due to ultrasound's simultaneous initiation of chemical (radical) and mechanical (vibrational)

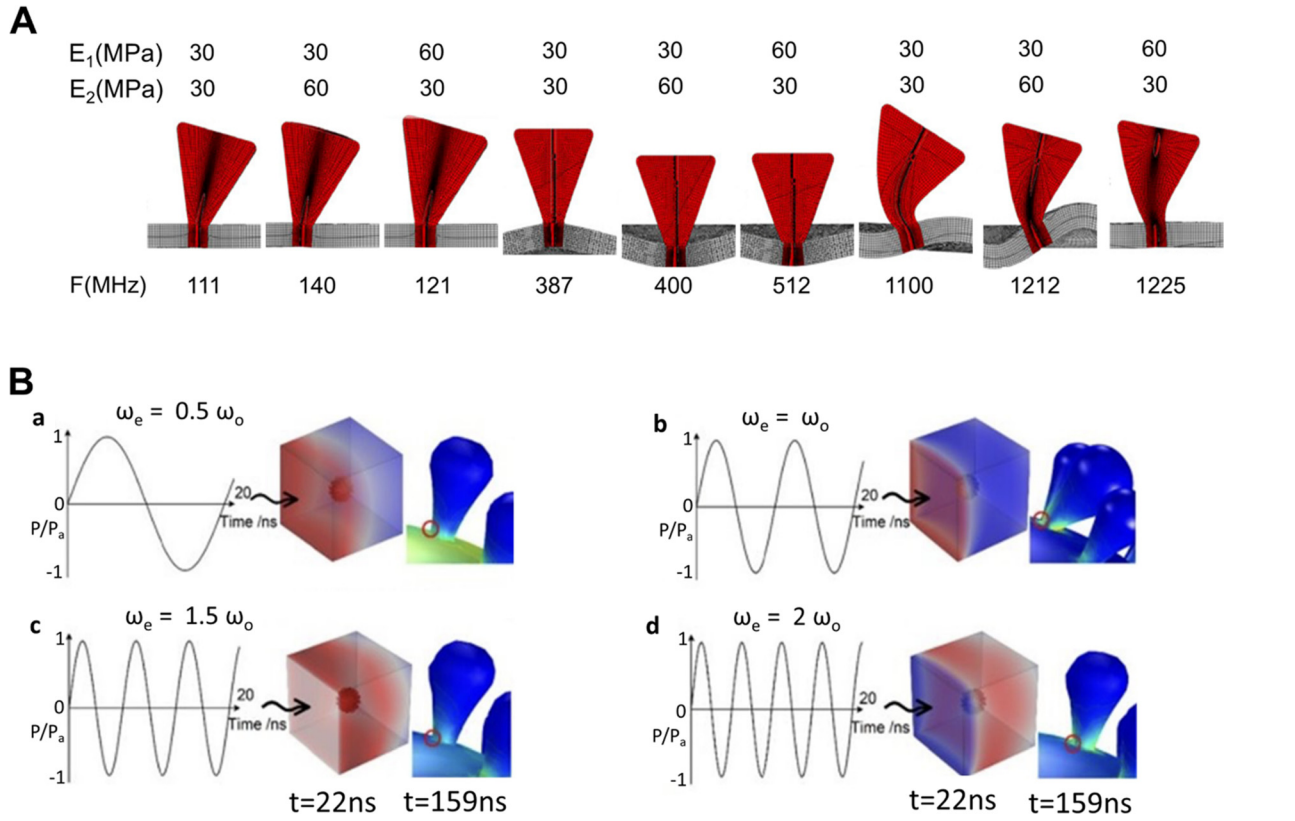

FIG. 3. The ultrasonic inactivation research highlights the method's effectiveness in precisely matching virus natural frequencies to mechanically damage their structure. (a) Sonomechanical effects and oscillating mode of low-frequency irradiations of ultrasound waves on the physical properties of SARS-CoV-2 spike and shell, as an airborne virus model. Reproduced with permission from Wierzbicki *et al.* J. Mech. Phys. Solids. **150**, 104369 (2021). Copyright 2021 Elsevier.[74] (b) Stress amplification at the viral spike root under ultrasound at single frequency ω_e relative to the virus's initial natural frequency ω_0, with (a) 0.5, (b) 1.0, (c) 1.5, and (d) 2.0 multipliers. Showcases the acoustic pressure, stress field, and ultrasonic wave profiles impacting the spike from 22 to 159 ns, highlighting the ultrasound's capacity to disrupt the viral structure through resonant frequency alignment. Reproduced with permission from Liu *et al.* Ultrasonics **124**, 106749 (2022). Copyright 2022 Elsevier.[76]

reactions, making it difficult to isolate the mechanical effects in the absence of radicals. Cavitation effects have been observed to mechanically fracture the cell membrane, as demonstrated through electron microscopy,[78] assumingly via protein or lipid damage of virus membrane. In contrast, some studies propose that ultrasound can disrupt the virus genome by mechanically fracturing sugar–phosphate bridges within the DNA through cavitation, as well as disrupting hydrogen bonds through radical reactions.[61]

In investigating the impact of mechanical cavitation on virus inactivation, Pförringer *et al.*[36] explored the use of CO_2 shielding gas to mitigate radical formation, focusing on the effects of frequency and power density. The study utilized four model viruses: BVDV and SFV (ssRNA enveloped, Hepatitis C models), PRV (herpes enveloped virus model), and PPV (non-enveloped B19 virus model) [Fig. 4(a)]. Factor VIII activity showed a 75% reduction after 300 min at 250 kHz highlighting the potential of vibrational anti-viral treatment for blood products without affecting coagulation factors [Fig. 4(b)]. However, adjusting power density to 1200 W and frequency to 27 kHz optimized virus inactivation with minimal blood factor effects [Fig. 4(c)], emphasizing the role of virus size and compactness in inactivation efficiency. Future investigations in this field should prioritize optimizing mechanical effects by identifying the precise natural frequency and power density, ensuring minimal adverse effects on blood products.

D. Matching ultrasound frequencies with natural resonance of virus structure

Viruses can be specifically inactivated by vibrating at GHz frequencies, leveraging a mechanism similar to microwave ovens' resonant absorption. This "virus resonance" suggests that viruses might absorb ultrasound energy at specific frequencies, leading to their deactivation.[28,79–82] Research into the vibrational modes of various viruses, including enveloped ones like HIV[83] and SARS-CoV-2,[74] supports this hypothesis, indicating a potential vulnerability to ultrasound vibrations.

The physical structure of viruses, including their shape and size, significantly influences their natural resonance frequency, crucial for cavitation's effectiveness. Viruses, with sizes ranging from 20 to 200 nm, are expected to have high resonant frequencies in the gigahertz range, differing notably from human cells due to their smaller dimensions and unique mechanical properties. This difference suggests that viruses can be inactivated at lower pressures compared to those

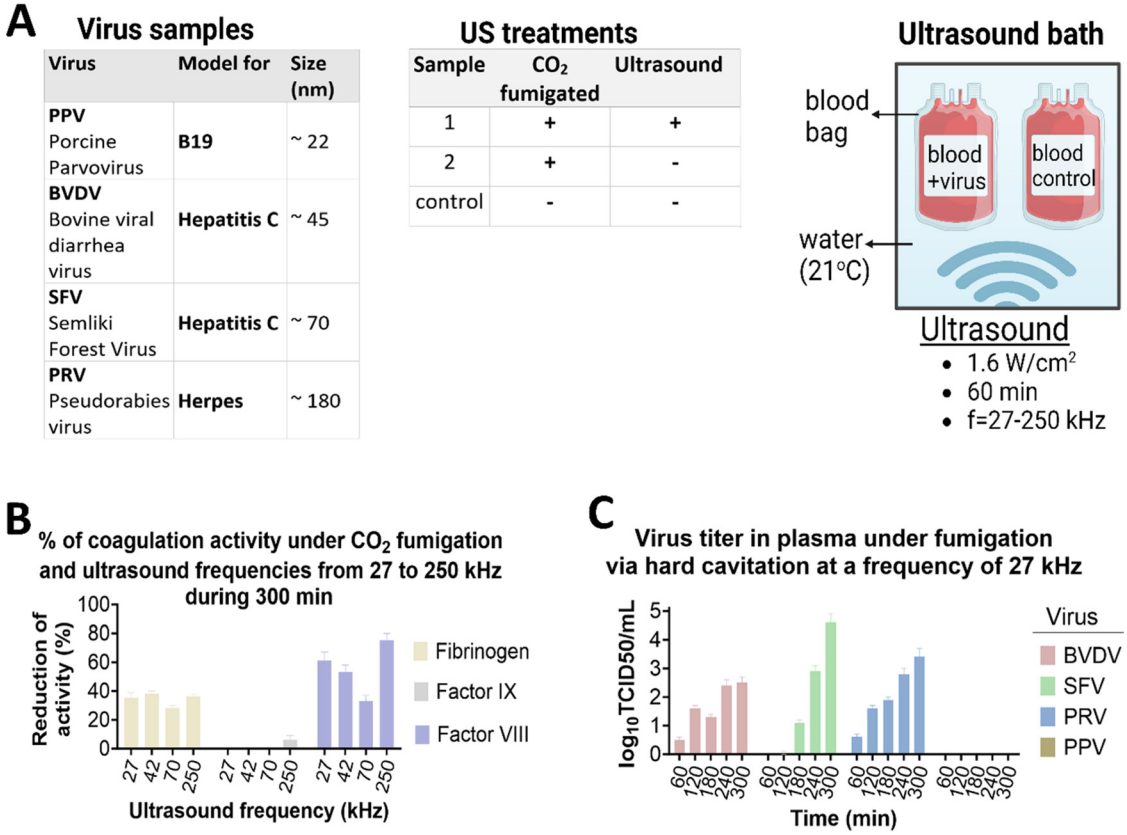

FIG. 4. Reduction of virus load in blood plasma due to mechanical cavitation. (a) The tables and schemes depict the sampling and methodology of CO_2 fumigation, to avoid radical reactions during sonication. (b) Extending the duration by 300 min and increasing the frequency by 250 kHz has adverse effects on the activity of plasma coagulation factors. (c) In the lowest frequency of 27 kHz, all virus models, except PPV, exhibit exposure time-dependent inactivation. Reproduced with permission from Pförringer *et al.* Euro. J. Med. Res. **25**, 12 (2020). Copyright 2020 Authors, licensed under a Creative Commons Attribution (CC BY) license.[36]

potentially harmful to cells. The efficiency of inactivating viruses like bacteriophages MS2 and ΦX174 varies with ultrasonic frequencies,[33] indicating structural variations affect inactivation mechanisms, possibly through shockwaves.[62]

The diameter of the coronavirus family is ∼100 nm packing ∼30-kb-long single-segmented RNA and with the spikes ∼20 nm in length.[77] These geometries are somewhat similar to other envelope viruses, such as HIV and influenza A viruses. Following a mechanochemical process, the spike protein first binds to a cell receptor through the RBD and then begins the fusion process.[77] Buehler and his team[84,85] studied the nanomechanical features of the spikes of coronavirus family. Their work showed the overall flexibility and mobility ratio of RBD have positive correlation with case fatality rate and inverse relationship with the virus infectivity. The results imply that the mechanical and structural properties of virus, specifically their vibrational spectrum and quantitative measures of mobility, could be linked directly to viral infectivity, offering potentially new strategies to inactivate virus. To enhance nanostructure reliability, it is important to have deeper mechanical analysis of virus envelope proteins[84,85] and ribonucleoproteins (RNPs), individually[86] or in interaction with cell receptor.[87]

Several theoretical models, such as Eringen's nonlocal theory,[88] and Buehler's machine learning model,[89,90] have been developed for better understanding of how natural vibrational frequencies of virus nanostructures relate to viral infectivity. Buehler and his team employed a graph neural network trained with structural data and normal mode frequencies for rapid prediction of natural vibrational frequencies of viral proteins based on their primary sequences.[89]

Using nonlinear continuous environment models, Eringen and Wegner[91] studied the vibrational behavior of nanosheets. By introducing a scale parameter, they also considered small-scale effects. Dastjerdi *et al.*,[92] employing Eringen's nonlocal elasticity theory, examined the deformations and natural frequencies of SARS-CoV-2, revealing resonance within the ranges of $3\,\text{GHz} < f1 < 4$ and $7\,\text{GHz} < f2 < 25\,\text{GHz}$ for the first and second natural frequencies, respectively. Given the virus's approximate radius of 100 nm, the interval for the first natural frequency (f1) could be smaller than a virus with 50 nm radius. Therefore, for the viruses with about 100 nm radius[77] (such as HIV, influenza, and SARS-CoV-2 virus), the distance between classical and nonlocal results is insignificant.[92] However, the average size and notable deviation observed in viral structures across simulation studies lead to uncertain natural frequency predictions, posing a

potential challenge for viral inactivation.[75] Moreover, the effects of the geometry deviation and environmental changes (such as temperature changes) on the natural vibration modes of a virion should be included in the investigation.

Resonance can occur when the irradiation frequency matches one of the natural frequencies of the system and can lead to severe mechanical damage. Hence, employing irradiation at the appropriate frequency could offer a novel approach to controlling virus transmission. The natural frequency of viral oscillations, determined by the chemical structure of each virus, is quite high compared to human cells. For example, HIV, hepatitis, and Ebola have natural frequencies of 18, 37, and 19 GHz, respectively.[93] A virus's genetic material is enclosed within the capsid. Two competing processes—transient vibration of the lipid membrane (coupled with resonant oscillations of individual spikes) and buckling/collapse of the entire capsid—can occur. Both processes generate significant tensile stresses, potentially leading to degradation and ruptures, thereby releasing RNA from the virus envelope. High frequencies (>30 MHz) can be achieved by using ultrasonic transducers to destroy the virus structure.[94] The frequency of ultrasonic waves can be adjusted to match the natural frequency of the virus so that capsid of a virus can be destroyed by mechanical irradiation for virus inactivation.[95] Ultrasonic waves directly stimulate the mechanical resonance of the virion, causing extensive deformation and rupture of its spikes or envelope, resulting in rapid virus deactivation. This mechanical resonance depends on the condition that the ultrasound wave frequency closely aligns with one of the natural frequencies of the viral spike or envelope.[48]

III. MICROWAVE AND RADIO WAVE

A. Non-thermal effects of microwave irradiation on virion in different media

Radiofrequency (RF) waves [3 kilohertz (kHz) to 300 megahertz (MHz)] and microwave (MW) [300 MHz to 300 gigahertz (GHz)] have been proven to inactivate microorganisms in solid, liquid, water phases, and a few studies on airborne microbes.[96] The question of whether RF irradiation can affect biological systems by non-thermal mechanisms has been an argumentative topic. Previous studies believe that microwave (MW) irradiation primarily exerted its disinfection effects through thermal mechanisms, causing denaturation and membrane damage within pathogens, thereby compromising their viability.[97] Nonetheless, recent studies have emerged suggesting the occurrence of non-thermal effects during MW-based disinfection of microorganisms.[98]

The disparity in outcomes between thermal and non-thermal microwave (MW) disinfection methods may stem from the differential interactions of MW photons with the medium.[98] As demonstrated by Wang *et al.*,[99] MW radiation exhibited a more pronounced inactivation effect on airborne bacteria compared to waterborne bacteria due to significant microwave energy absorption by water. This differentiation between thermal effects on waterborne bacteria and non-thermal effects on airborne bacteria informs our understanding of how microwaves interact with pathogens,[100] including viruses in different media.

In the last few decades, several researchers have outlined air or water-mediated non-thermal effects of MWs on free ions, biomolecules, and biochemical reactions within biological systems.[98,101–103] In the context of non-thermal MW irradiation for virus inactivation, particularly within the coronavirus family, successful results have been observed in aerosol[39] and liquid media;[38] however, the inactivation of coronaviruses on dry surface may not be clinically significant,[40] indicating the importance of considering specific conditions and media for effective virus inactivation.

Researchers at the United States Air Force Research Laboratory developed an apparatus for controlled microwave exposure of aerosolized virus and explored the role of air media in virus inactivation. They developed experimental instruments to deliver electromagnetic waves to an aerosol mixture of biological medium and aerosolized SARS-CoV-2, adjusting the strength, energy, and frequency of irradiation[103,104] [Fig. 5(a)]. To simulate airborne pathogens, the researchers exposed a harmless human coronavirus surrogate, bovine coronavirus, to various microwave waveforms ranging from 2.8 to 7.5 GHz. The resulting system was designed to examine both resonant (frequency-dependent) excitation of mechanical modes in the virus, leading to fatigue failure, and thermal heating, which exhibits slight frequency dependence but is distinct from resonance associated with mechanical modes.[103,104] At a core frequency of 4.2 GHz, the system uses a gyromagnetic nonlinear C-band transmission line source with a peak power of up to 80 kW, achieving RF electric field strengths of up to 280 kV/m (17%) within the aerosol flow zone of the RF exposure device.[104] Using this apparatus, the authors demonstrated that applying a 5.6 GHz, 4.8 kHz repetition rate RF waveform to aerosolized BCoV resulted in an inactivation rate of approximately 74% in aerosol stream.[105]

As a model of water-mediated surrounding environment, Yang *et al.*[37] investigated the non-thermal effects of microwaves on H3N2 virus suspended in the culture media. The efficiency of such energy transfer was explored through the virus inactivation ratio measurements. At the resonant frequency, H3N2 virus inactivation was observed by illuminating 8 GHz microwaves at 82 W/m^2, generating an average 86.9 V/m electric field intensity inside the solution [Fig. 5(b)]. However, to ensure controlled non-thermal conditions during non-thermal MW irradiation, it is crucial to minimize local thermal effects caused by liquid media. This helps establish that inactivation primarily results from electromechanical forces disrupting the viral membrane. For heat-controlled investigations, the virion can be in aerosolized form with minimal liquid in the droplet, or the virus suspension droplet can be dried on a surface, as demonstrated by Cantu *et al.*[27] and Echchgadda *et al.*[40] using a plastic coverslip containing BCoV virus for surface drying [Fig. 5(c)].

Beside the media, the intensity and frequency of MW play the key roles in non-thermal disinfection. Several studies have compared the pathogen inactivation potency using different MW modulated radiations high or low frequency or in continuous flux of waves (CW).[101,102] Typically, the studies on MW-based inactivation of pathogens have been performed in the S-band at or around 2.45 GHz using CW, however, theoretically the long-time exposure (quasi-CW) might also lead to inactivation[103] [Fig. 5(a)]. Betti *et al.*[101] studied the effects of non-thermal MW irradiation on tobacco plants infected with tobacco mosaic virus (TMV). They used a device producing weak intensity microwave beams (10^{-12} W cm^{-2}) in CW or modulated frequency (10, 100, and 1000 Hz) coupled with red/near-infrared radiation. Low-frequency modulation showed higher bioactivity, especially in indirect water-mediated treatments, but the study did not demonstrate the effect of MW irradiation on viral activity.[102]

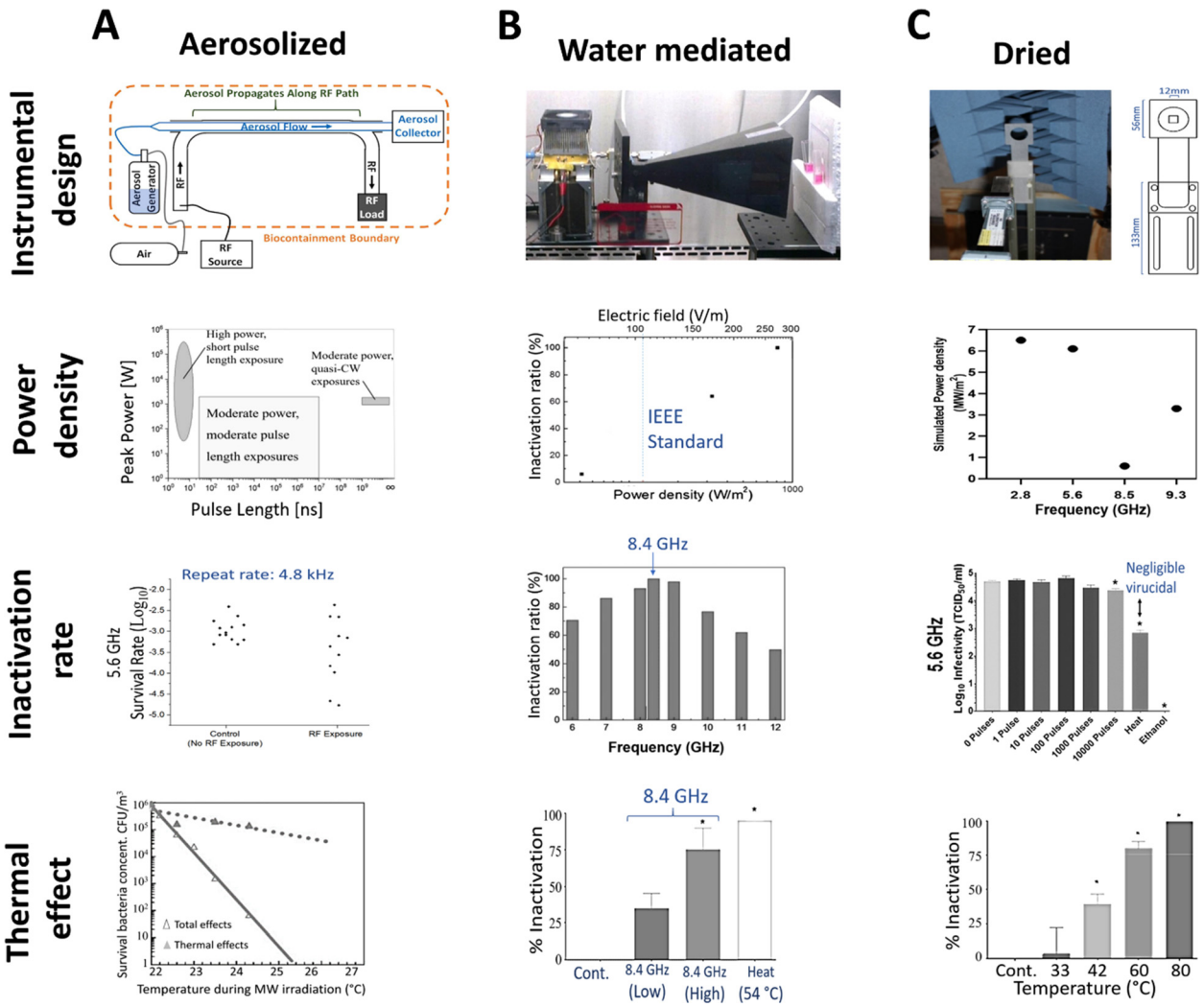

FIG. 5. The media surrounding virion, as well as the intensity and frequency of MW play the key roles in non-thermal MW disinfection. The instruments generating virion surrounded by appropriate media are demonstrated here. In the lack of appropriate heat control, the thermal effect dominates inactivation in water/dry media, with negligible impact on airborne viruses. (a) Conceptual schematic illustrating critical components of the viral aerosol microwave inactivation experiment. Reproduced with permission from Hoff *et al.*, Rev. Sci. Instrum. **92**, 014707 (2021). Copyright 2021 AIP Publishing.[104] Three distinct exposure regimes: long-time (quasi-CW) and high-peak power, short-pulse, were explored at 5.6 GHz with pulse repetition rate at 4.8 kHz. Reproduced with permission from Enderich *et al.*, Rev. Sci. Instrum. **92**, 064712 (2021). Copyright 2021 AIP Publishing.[103] Thermal effects account for total inactivation of airborne pathogen under MW irradiation, solid line (MW + thermal) vs dashed line (thermal only). Reproduced with permission from Wang *et al.*, J. Aerosol Sci. **137**, 105437 (2019). Copyright 2019 Elsevier.[99] (b) Effect of 8 GHz microwave resonance on H3N2 virus inactivation in a water-based solution, demonstrating a robust resonance effect at 8.4 GHz with an average 86.9 V/m electric field that leads in 100% inactivation induced by structure-resonant energy transfer (SRET). Reproduced with permission from Yang *et al.*, Sci. Rep. **5**, 18030 (2016). Copyright 2016 Authors, licensed under a Creative Commons Attribution (CC BY) license.[37] However, the accuracy of inactivation measurement may be influenced by high-power (30 W applied) exposure due to elevated local heat from surrounding media.[27] (c) Virus inactivation on the dry surface at 8.4 GHz exhibits the lowest power density of 0.6 MW/m^2, compared to 6.1 MW/m^2 at 5.6 GHz. Reproduced with permission from Echchgadda *et al.*, Bioelectromagnetics **44**, 5–16 (2023). Copyright 2023 Wiley-VCH.[40] Increasing pulse number beyond 10 000 pulses does not further enhance viral inactivity at 5.6 GHz. Control tests at 33 °C for 15 min show negligible thermal-mediated inactivation. Reproduced with permission from Cantu *et al.*, Sci. Rep. **13**, 9800 (2023). Copyright 2023 Authors, licensed under a Creative Commons Attribution (CC BY) license.[27]

Thermal effects play a significant role in the inactivation of viruses in air, water, and dry media when exposed to microwave irradiation. Thermal mechanisms predominantly inactivate waterborne pathogens, whereas non-thermal mechanisms are more crucial for airborne pathogen sterilization. Minimal temperature changes during MW irradiation for airborne pathogens, such as bacteria,[99] underscore the importance of non-thermal processes. Similar to airborne bacteria, the aerosolized viruses exposed to 5.6 GHz experience substantial inactivation, with non-thermal effects leading the process[103,105] [see the thermal effect in Fig. 5(a)]. In contrast, virus inactivation in a water-based solution at 8 GHz with high-power exposure (30 W applied) should be considered due to elevated local heat from surrounding

media[27] [Fig. 5(b)]. In the dry media, virus inactivation on a dry surface at 8.4 GHz exhibits a lower power density of 0.6 MW/m^2 compared to 6.1 MW/m^2 at 5.6 GHz.[40] Heat control tests at 33 °C for 15 min show negligible thermal-mediated inactivation[27] [Fig. 5(c)]. Observations suggest possible thermal and spike protein orientation-related mechanisms, and further tests should model the nanoscale thermal environment during RF exposure and analyze spike protein orientation within viral particles using FRET or Raman methods for confirmation.

In the absence of heat regulation, microwave irradiation can interact with protein charges, potentially breaking bonds and denaturing the protein structure more effectively than heat alone. It can disrupt the hydrogen bond network of water molecules,[106] affecting intermolecular modes and promoting protein-water H-bond breakdown and deformation.[107] Studies on SARS-CoV-2 spike protein has also been shown that microwave irradiation can cause considerable denaturation from 2 to 10 min at body temperature (37 °C). Exposing spike protein to a 700 W, 2.45 GHz electromagnetic field for 2 min resulted in approximately 95% protein denaturation, a level comparable to thermal denaturation at 75 °C for 40 min.[26]

The uncontrolled heat due to the RF irradiation can not only affect negatively on the viral protein, such as capsid, spike, or envelope protein, but also the viral genome. The investigation of electromagnetic fields (EMFs) on SARS-CoV-2 revealed that the viral genome, particularly the RNA, exhibits a substantial dipole moment, making it highly reactive to High Frequency EMFs.[108] Unlike cells, the viral RNA is not bound in histones, allowing it to move freely and be affected by EMFs with resonant frequencies detectable by spectroscopic detection of phosphate bands. Vibrational bands associated with the viral capsid and phosphate oscillatory bands on the genome were studied using infrared spectroscopy, highlighting their vulnerability to EMFs.[109] Amplification at a resonant frequency could lead to detrimental effects on each viral structure, ultimately leading to viral destruction. Proper control of thermal effects during EMF irradiation is crucial to harness this potential for therapeutic and sanitation applications in combating viral infections. This highlights the importance of precise thermal effect control in ensuring the effectiveness of non-thermal microwave irradiation, as uncontrolled heat may lead to undesirable consequences.

B. Identification of frequencies matching with the dipolar confined-acoustic vibrations (CAVs) mode of virus

As explained above, once a resonant frequency is determined for one of the structures of a virus, the electromagnetic field (EMF) irradiation at that frequency can be used to inactivate the virion. With an observed inactivation threshold at a microwave power density that is within the safety standard of IEEE, the uncovered structure resonance energy transfer (SRET)[37] mechanism can pave the way for the development of a novel strategy to prevent airborne virus epidemics in the public. According to the International Commission on Non-Ionizing Radiation Protection (ICNIRP), the non-thermal public safety limit for 100 kHz–300 GHz is 200 W/m^2 absorbed power density. Cells can withstand power densities of nonionizing radiation of 50–150 W/m^2 during therapeutic interventions without cellular stress or thermal effects.[20]

By measuring the viral inactivation threshold, it was proposed to investigate the efficiency of SRET from MWs on viruses. In a study investigating the inactivation ratio of influenza A (H3N2) virus using MWs, the model examined dipolar-mode resonance and off resonance microwave frequencies across varying microwave powers.[37] Results revealed a robust resonance effect on virus inactivation ratio at the dipolar oscillation frequency of 8.4 GHz,[37] suggesting the observed virus inactivation post-microwave irradiation is attributed to the proposed SRET effect [Fig. 5(b)]. Moreover, they detected inactivation of the H3N2 virus at the resonant frequency by irradiating the viral solution with 82 W/m^2 (lower than the IEEE public space safety standard) of 8 GHz microwaves, which corresponds to an average electric field strength of 87 V/m within the solution. This validates the accuracy of the proposed model in estimating the field threshold (86.9 V/m) for structural fracturing of the virus. Furthermore, investigation into virus inactivation at non-resonant frequencies (6–12 GHz) with a low resonator quality factor (less than 2 for H3N2) was conducted, as predicted by the model.

Similar to Influenza virus, the SARS-CoV-2 coronavirus can resonate in the dipolar confined acoustic vibrations (CAVs) mode when exposed to microwaves of the same frequency, resulting in inactivation at a reasonable microwave power density deemed safe for public exposure.[22,32] Barbora and Minnes.[22] proposed a technique to selectively inactivate virus particles by inducing forced oscillations through SRET, thereby diminishing infectivity and disease advancement. Their research revealed that the optimal resonant frequencies for various forms of SARS-CoV-2 ranged from 10 to 17 GHz[22] with simultaneous irradiations at 14.5 ± 1 W/m^2. This dose is below the 200 W/m^2 safety standard defined by the ICNIRP, for 100% inactivation of SARS-CoV-2 virus particles in the throat-lung lining.

C. Factors affecting microwave resonant absorption (MRA) of virus

Microwaves of the same frequency through microwave resonant absorption (MRA) effect can resonantly excite the dipolar mode of the confined acoustic vibrations (CAVs) inside virions.[28,37,110] MRA can be affected by virus attributes including hydration level, surface charge, and size. For example, the hydration levels on the virus capsid can affect the bandwidth of CAV-induced MRA.[110] Moreover, medium surrounding the virion, such as water or air, may affect the MRA. By increasing the absorbed charges on the surface of virions, the magnitude of MRA will be enhanced and then suppressed when virions reach isoelectric points.[28] Size of virus is another critical factor affecting the MRA magnitude. Bigger virus has smaller MRA magnitude. In one study, Liu *et al.*[28] showed the spherical influenza A virions with −11 mV zeta potential and 93 nm hydrodynamic diameter have a resonant absorption frequency peak around 12 GHz. In contrast, the spherical enterovirus-71 virions which have smaller size with more charge surface (−25 mV, and 40 nm hydrodynamic diameter) diameter have a resonant absorption frequency peak around 44 GHz, which reflecting the expected size and charge dependency.[28] These observations also confirm the dipolar CAVs of virions can, indeed, cause MRA.

Size distribution of virion and its surrounding medium are the other two factors affecting the quality factor of the microwave resonant absorption (QMRA).[32,110,111] Wang *et al.*[32] designed a sensing device using coplanar waveguide (CPW) to study virions' resonant

frequencies. For SARS-CoV and SARS-CoV-2, they observed two significant MRA peaks at 4 and 7.5 GHz, respectively, with a relatively large bandwidth. The resonant frequencies inversely correlate with virion diameter, leading to a broader range of frequencies [Fig. 2(g)].

Another factor influencing QMRA is the surrounding medium. Viscous water can dampen mechanical vibrations, decreasing the quality factor of the first dipole. Similar QMRA values in the same medium were observed for HCoV-229E and SARS-CoV-2, structurally similar viruses.[32]

However, changing the medium's pH from neutral to acidic reduced the absorption efficiency for both MRA peaks. The second MRA peak showed a shift from 7.6 to 7.8 GHz in acidic media, attributed to increased zeta potential from surface charges. This observation is significant for virus sampling from saliva[112] and respiratory mucosa,[113] which have an average pH value of 6.7, impacting the resonant frequency of virions induced by SRET.

Contrasting observations on various viruses highlight complex interactions with RF fields, suggesting a broad resonant frequency or alternative inactivation mechanisms. Cantu *et al.*[27] and Echchgadda *et al.*[40] noted that while they could not definitively prove the occurrence of SRET in BCoV upon exposure to RF fields, they did observe a 60%–70% inactivation of BCoV following a similar exposure paradigm. They speculated that the differences observed between their study and Wang *et al.*'s previous work[32] might be attributed to variations in the virion species itself, such as the larger size and mass of their virus, leading to a shift in resonant frequencies. In contrast, Wang *et al.*[32] reported noticeable microwave absorption and identified resonant frequencies of the first and second dipolar modes of SARS-CoV-2 as 4 and 7.5 GHz, respectively [Fig. 2(g)].

The SRET effect from microwaves to viral CAVs in a water-based solution was studied, and its efficiency was measured by the viral inactivation rate.[19,32,37] The research proposed a damped mass-spring model and experimentally determined the microwave absorption cross section of a single virus to predict the required electric field magnitude for virus destruction at different illumination frequencies.[37] The inactivation ratio peaked at the resonance frequency of dipolar resonance after microwave irradiation, with physical destruction of viruses observed without altering the viral RNA genome. This novel energy transfer mechanism between RF waves and viruses demonstrates the feasibility of the SRET effect in virus inactivation. Furthermore, resonance effects elicited different biological responses in different samples due to changes in biochemical composition and membrane-induced charge separation.[21,114] Microwave radiation at GHz frequencies can disrupt the directional arrangement of water molecules and hydrogen bonding networks around biomolecules, impacting their properties, and consequent viral protein deformation.[114] This effect is enhanced by endoscopic medical instruments with high frequency (SHF) (3–30 GHz),[22] enabling nonthermal SRET-mediated inactivation of SARS-CoV-2 in deep tissues, offering a potential strategy for future viral pandemics.

D. Deciphering the virus's innate "musical signature" through modeling and numerical experiments

Due to the differences between biological systems, such as cells and viruses, the natural resonant frequencies of human cells are expected to differ from those of viruses. Therefore, using a non-ionizing wave that is specific to match the resonance frequency of SARS-CoV-2 can protect humans from the harmful effects of electromagnetic waves. Based on such a hypothesis, the electromagnetic radiation at a SARS-CoV-2 resonance frequency can penetrate deep into the human body and alters virus.[109] As discussed above, the SRET effect from MWs to viral CAVs can be efficient enough to swing mechanically the spike in a specific vibrational signature of virus resulting in virus inactivation. This vibrational signature of virus inherent in such an ensemble of spike proteins.[115] The mechanical properties of spike, such as mode shapes and natural frequencies, have been predicted using the molecular dynamic (MD) simulation. The frequencies are shown to be within the safe range of 1–20 MHz routinely used for medical imaging and diagnosis by means of ultrasound.[116] The frequencies are in consistent with the previous report[74,117] predicting the existence of three distinct resonant frequencies of 111 MHz for the individual spike.

In parallel, numerical experiments have unveiled the natural frequencies associated with the swinging motion of the SARS-CoV-2 spike, falling within the ranges of (0.07 and 0.12 GHz) or (0.26 and 0.44 GHz), accounting for potential temperature elevations.[76] These natural frequencies are virus's innate "musical signature," which particularly make the spike swings and physically fracturing the virus structure. Remarkably, even with emerging mutants, the spike vibration pattern remains consistent, resulting in corresponding musical signatures falling within specific ranges of spike oscillation.[76]

IV. CONCLUSION AND FUTURE PROSPECTIVE

Novel physical strategies like ultrasound and non-thermal microwaves hold promise for virus inactivation, targeting specific virion structures' resonant frequencies without harming human cells or the environment, a feat unattainable with conventional methods. Ultrasound-induced cavitation exploits mechanical and chemical reactions, while microwave-assisted inactivation disrupts virion structures through beneficial non-thermal effects and structural resonance energy transfer (SRET) phenomena. Surrounding medium (air, liquid, or dry) and structural features of irradiated virus, such as size, shape, and surface adherence, can influence the efficiency of virus inactivation. Leveraging vibrational resonance frequencies offers innovative pathways for virus control and public health.

In the future, advancements in technologies for viral inactivation through matching vibrational resonance will require further investigation, particularly focusing on the precise identification of natural frequencies for various viral strains and elucidating the underlying mechanisms. Novel theoretical research like quantum tunneling,[118] machine learning,[89,90] and computational modelling[92,116,119] might shed light on the vibrational mode of virion and its structural–acoustic interactions, aiding future experimental studies. This understanding will enhance the development of targeted resonance-based therapies, promising effective viral neutralization while minimizing harm to human body. Emerging nanophotonics techniques, such as quantum measurement[120] and cavity-enhanced single-particle spectroscopies,[55,121] facilitate characterizing the resonant frequencies of different types of viruses. In addition, compiling these data into a comprehensive database[122,123] of vibrational fingerprints can be a new direction of research for applied physics community to contribute to modern microbiology and virology.

Current research in this field primarily focuses on virions, the cell-free form of viruses, due to their complex mechanisms. However, the future studies should explore the complex interactions between

viruses and cells, as well as the replication and transcription of pathogenic viruses, during and after exposure to sound or electromagnetic waves. This deeper knowledge is crucial for extending this technology beyond virion inactivation to inhibiting virus propagation within infected cells.

In the field of viral inactivation using ultrasound, current research predominantly emphasizes acoustic cavitation, especially in liquid media. A significant challenge remains in developing effective cavitation generation methods adjusted with the media and deciphering cavitation's possible effects, including mechanical, thermal, and chemical effects, as this knowledge will help the targeted anti-viral therapy without harming surrounding cells. Understanding how irradiation affects viral structures in their surrounding environment and the potential for viral recovery after non-thermal processes is crucial for assessing virus inactivation efficacy and guiding future diagnostic and treatment approaches.[124] Whether for ultrasound or radio frequency radiation, precisely tuning exposure settings, including power density and magnitude, as well as media conditions and local heat, become essential to prevent adverse thermal effects and achieve optimal outcomes of controlled inactivation.

In the context of radio frequency waves, future research should focus on understanding mechanisms, like energy utilization, nonthermal effects, and SRET interactions between waves and viruses. To reach this aim, experimental studies must explore strategies to reduce excessive energy absorption by polar molecules and investigate the effects of varying electromagnetic wave frequencies on different viruses. Moreover, the future research should be directed toward accurately characterizing the natural frequencies of viruses, enabling the selection of the most effective destructive vibration mode. Identifying the matched frequency between the microwave and the virus confined-acoustic dipolar mode frequencies is vital for successful virus inactivation.

ACKNOWLEDGMENTS

This work was financially supported by the Australian Research Council Future Fellowships (Grant No. FT220100018), the Australian Research Council Center of Excellence for Quantum Biotechnology (Grant No. CE230100021), the National Health and Medical Research Council Investigator Fellowship—(Grant No. APP2017499), and the Australian Research Council Laureate Fellowship 2021 (Grant No. FL210100180).

AUTHOR DECLARATIONS

Conflict of Interest

The authors have no conflicts to disclose.

Author Contributions

Mohammad Sadraeian: Conceptualization (equal); Data curation (equal); Formal analysis (equal); Investigation (equal); Methodology (equal); Writing – original draft (equal); Writing – review & editing (equal). **Irina Kabakova:** Data curation (equal); Formal analysis (equal); Funding acquisition (equal); Investigation (equal); Writing – review & editing (equal). **Jiajia Zhou:** Conceptualization (equal); Data curation (equal); Formal analysis (equal); Supervision (equal); Validation (equal); Writing – original draft (equal); Writing – review & editing (equal). **Dayong Jin:** Conceptualization (equal); Data curation (equal); Formal analysis (equal); Funding acquisition (equal); Investigation (lead); Methodology (equal); Project administration (lead); Supervision (lead); Validation (equal); Visualization (equal); Writing – review & editing (lead).

DATA AVAILABILITY

The data that support the findings of this study are available from the corresponding authors upon reasonable request.

REFERENCES

[1]F. Tarendeau *et al.*, "Structure and nuclear import function of the C-terminal domain of influenza virus polymerase PB2 subunit," Nat. Struct. Mol. Biol. **14**, 229–233 (2007).
[2]M. A. Garcia-Blanco and B. R. Cullen, "Molecular basis of latency in pathogenic human viruses," Science **254**, 815–820 (1991).
[3]J. Louten, "Virus structure and classification," *Essential Human Virology* (Elsevier, 2016), Vol. 19.
[4]R. Wyatt and J. Sodroski, "The HIV-1 envelope glycoproteins: Fusogens, antigens, and immunogens," Science **280**, 1884–1888 (1998).
[5]W. T. Harvey *et al.*, "SARS-CoV-2 variants, spike mutations and immune escape," Nat. Rev. Microbiol. **19**, 409–424 (2021).
[6]M. Letko, A. Marzi, and V. Munster, "Functional assessment of cell entry and receptor usage for SARS-CoV-2 and other lineage B betacoronaviruses," Nat. Microbiol. **5**, 562–569 (2020).
[7]A. Almeida, M. A. F. Faustino, and M. G. Neves, "Antimicrobial photodynamic therapy in the control of COVID-19," Antibiotics **9**, 320 (2020).
[8]H. Majiya, O. O. Adeyemi, M. Herod, N. J. Stonehouse, and P. Millner, "Photodynamic inactivation of non-enveloped RNA viruses," J. Photochem. Photobiol., B **189**, 87–94 (2018).
[9]D. Schuster, C. Laggner, and T. Langer, "Why drugs fail—A study on side effects in new chemical entities," Curr. Pharm. Des. **11**, 3545–3559 (2005).
[10]S. A. Amin, S. Banerjee, K. Ghosh, S. Gayen, and T. Jha, "Protease targeted COVID-19 drug discovery and its challenges: Insight into viral main protease (Mpro) and papain-like protease (PLpro) inhibitors," Bioorg. Med. Chem. **29**, 115860 (2021).
[11]F. G. Njoroge, K. X. Chen, N.-Y. Shih, and J. J. Piwinski, "Challenges in modern drug discovery: A case study of boceprevir, an HCV protease inhibitor for the treatment of hepatitis C virus infection," Acc. Chem. Res. **41**, 50–59 (2008).
[12]M. Sadraeian, L. Zhang, F. Aavani, E. Biazar, and D. Jin, "Viral inactivation by light," eLight **2**, 18 (2022).
[13]M. Sadraeian, L. Zhang, F. Aavani, E. Biazar, and D. Jin, "Photodynamic viral inactivation assisted by photosensitizers," Mater. Today Phys. **28**, 100882 (2022).
[14]M. Gennady *et al.*, "Photodynamic action in thin sensitized layers: Estimating the utilization of light energy," J. Biomed. Photonics Eng. **7**, 40301 (2021).
[15]F. Alves *et al.*, "Strategies to improve the antimicrobial efficacy of photodynamic, sonodynamic, and sonophotodynamic therapies," Lasers Surg. Med. **53**, 1113–1121 (2021).
[16]A. E. Powles, D. J. Martin, I. T. Wells, and C. R. Goodwin, "Physics of ultrasound," Anaesth. Intensive Care Med. **19**, 202–205 (2018).
[17]W. Duco, V. Grosso, D. Zaccari, and A. T. Soltermann, "Generation of ROS mediated by mechanical waves (ultrasound) and its possible applications," Methods **109**, 141–148 (2016).
[18]N. Wang, W. Zou, X. Li, Y. Liang, and P. Wang, "Study and application status of the nonthermal effects of microwaves in chemistry and materials science–a brief review," RSC Adv. **12**, 17158–17181 (2022).
[19]International Commission on Non-Ionizing Radiation Protection (ICNIRP), "Guidelines for limiting exposure to electromagnetic fields (100 kHz to 300 GHz)," Health Phys. **118**, 483–524 (2020).
[20]M. Zhadobov, N. Chahat, R. Sauleau, C. Le Quement, and Y. Le Drean, "Millimeter-wave interactions with the human body: State of knowledge and recent advances," Int. J. Microwave Wireless Technol. **3**, 237–247 (2011).

[21]K. Komoshvili *et al.*, "W-band millimeter waves targeted mortality of H1299 human lung cancer cells without affecting non-tumorigenic MCF-10A human epithelial cells in vitro," Appl. Sci. **10**, 4813 (2020).
[22]A. Barbora and R. Minnes, "Targeted antiviral treatment using Non-ionizing radiation therapy for SARS-CoV-2 and viral pandemics preparedness: Technique, methods and practical notes for clinical application," PLoS One **16**, e0251780 (2021).
[23]X. Xiong *et al.*, "A thermostable, closed SARS-CoV-2 spike protein trimer," Nat. Struct. Mol. Biol. **27**, 934–941 (2020).
[24]C. R. Arbeitman, P. Rojas, P. Ojeda-May, and M. E. Garcia, "The SARS-CoV-2 spike protein is vulnerable to moderate electric fields," Nat. Commun. **12**, 5407 (2021).
[25]Z. Kuang *et al.*, "Molecular dynamics simulations explore effects of electric field orientations on spike proteins of SARS-CoV-2 virions," Sci. Rep. **12**, 12986 (2022).
[26]P. Afaghi, M. A. Lapolla, and K. Ghandi, "Denaturation of the SARS-CoV-2 spike protein under non-thermal microwave radiation," Sci. Rep. **11**, 23373 (2021).
[27]J. C. Cantu *et al.*, "Evaluation of inactivation of bovine coronavirus by low-level radiofrequency irradiation," Sci. Rep. **13**, 9800 (2023).
[28]T.-M. Liu *et al.*, "Microwave resonant absorption of viruses through dipolar coupling with confined acoustic vibrations," Appl. Phys. Lett. **94**, 043902 (2009).
[29]X. Zhao, G. Dong, and C. Wang, "The non-thermal biological effects and mechanisms of microwave exposure," Int. J. Radiat. Res. **19**, 483–494 (2021).
[30]K. Yasui, *Acoustic Cavitation and Bubble Dynamics*, SpringerBriefs in Molecular Science (Springer, 2018), Chap. 1, pp. 1–35.
[31]Z. Ke *et al.*, "Structures and distributions of SARS-CoV-2 spike proteins on intact virions," Nature **588**, 498–502 (2020).
[32]P.-J. Wang *et al.*, "Microwave resonant absorption of SARS-CoV-2 viruses," Sci. Rep. **12**, 12596 (2022).
[33]C. V. Chrysikopoulos, I. D. Manariotis, and V. I. Syngouna, "Virus inactivation by high frequency ultrasound in combination with visible light," Colloids Surf., B **107**, 174–179 (2013).
[34]A. Sarkinas *et al.*, "Inactivation of some pathogenic bacteria and phytoviruses by ultrasonic treatment," Microb. Pathog. **123**, 144–148 (2018).
[35]N. Lu *et al.*, "Effect of ultrasound with methylene blue as sound sensitive agent on virus inactivation," Med. Novel Technol. Devices **17**, 100204 (2023).
[36]D. Pförringer *et al.*, "Novel method for reduction of virus load in blood plasma by sonication," Eur. J. Med. Res. **25**, 12 (2020).
[37]S.-C. Yang *et al.*, "Efficient structure resonance energy transfer from microwaves to confined acoustic vibrations in viruses," Sci. Rep. **5**, 18030 (2015).
[38]H. Banting, I. Goode, C. E. G. Flores, C. C. Colpitts, and C. E. Saavedra, "Electromagnetic deactivation spectroscopy of human coronavirus 229E," Sci. Rep. **13**, 8886 (2023).
[39]A. Manna *et al.*, "SARS-CoV-2 inactivation in aerosol by means of radiated microwaves," Viruses **15**, 1443 (2023).
[40]I. Echchgadda *et al.*, "Evaluation of viral inactivation on dry surface by high peak power microwave (HPPM) exposure," Bioelectromagnetics **44**, 5–16 (2023).
[41]B. Z. Fite, J. Wang, P. Ghanouni, and K. W. Ferrara, "A review of imaging methods to assess ultrasound-mediated ablation," BME Front. **2022**, 9758652.
[42]J. L. Paris and M. Vallet-Regí, "Ultrasound-activated nanomaterials for therapeutics," Bull. Chem. Soc. Jpn. **93**, 220–229 (2020).
[43]R. Chandan, S. Mehta, and R. Banerjee, "Ultrasound-responsive carriers for therapeutic applications," ACS Biomater. Sci. Eng. **6**, 4731–4747 (2020).
[44]T. Mason, E. Joyce, S. Phull, and J. Lorimer, "Potential uses of ultrasound in the biological decontamination of water," Ultrason. Sonochem. **10**, 319–323 (2003).
[45]P. Piyasena, E. Mohareb, and R. McKellar, "Inactivation of microbes using ultrasound: A review," Int. J. Food Microbiol. **87**, 207–216 (2003).
[46]P. R. Gogate, "Application of cavitational reactors for water disinfection: Current status and path forward," J. Environ. Manage. **85**, 801–815 (2007).
[47]D. J. Flannigan and K. S. Suslick, "Plasma formation and temperature measurement during single-bubble cavitation," Nature **434**, 52–55 (2005).
[48]N. S. M. Yusof, S. Anandan, P. Sivashanmugam, E. M. Flores, and M. Ashokkumar, "A correlation between cavitation bubble temperature, sonoluminescence and interfacial chemistry–A minireview," Ultrason. Sonochem. **85**, 105988 (2022).
[49]Z. Xu, T. L. Hall, E. Vlaisavljevich, and F. T. Lee, Jr., "Histotripsy: The first noninvasive, non-ionizing, non-thermal ablation technique based on ultrasound," Int. J. Hyperthermia **38**, 561–575 (2021).
[50]K. M. Imran *et al.*, "Magic bubbles: Utilizing histotripsy to modulate the tumor microenvironment and improve systemic anti-tumor immune responses," Int. J. Hyperthermia **40**, 2244206 (2023).
[51]K. J. Pahk, P. Gélat, H. Kim, and N. Saffari, "Bubble dynamics in boiling histotripsy," Ultrasound Med. Biol. **44**, 2673–2696 (2018).
[52]S. Li, Y. Wei, B. Zhang, and X. Li, "Research progress and clinical evaluation of histotripsy: A narrative review," Ann. Transl. Med. **11**, 263 (2023).
[53]Z. Izadifar, P. Babyn, and D. Chapman, "Ultrasound cavitation/microbubble detection and medical applications," J. Med. Biol. Eng. **39**, 259–276 (2019).
[54]L. Fan, A. I. Muhammad, B. B. Ismail, and D. Liu, "Sonodynamic antimicrobial chemotherapy: An emerging alternative strategy for microbial inactivation," Ultrason. Sonochem. **75**, 105591 (2021).
[55]S.-J. Tang *et al.*, "Single-particle photoacoustic vibrational spectroscopy using optical microresonators," Nat. Photonics **17**, 951–956 (2023).
[56]M. Zupanc *et al.*, "Effects of cavitation on different microorganisms: The current understanding of the mechanisms taking place behind the phenomenon. A review and proposals for further research," Ultrason. Sonochem. **57**, 147–165 (2019).
[57]N. S. M. Yusof *et al.*, "Physical and chemical effects of acoustic cavitation in selected ultrasonic cleaning applications," Ultrason. Sonochem. **29**, 568–576 (2016).
[58]T. Yusaf, "Experimental study of microorganism disruption using shear stress," Biochem. Eng. J. **79**, 7–14 (2013).
[59]K. R. Wigginton, B. M. Pecson, T. Sigstam, F. Bosshard, and T. Kohn, "Virus inactivation mechanisms: Impact of disinfectants on virus function and structural integrity," Environ. Sci. Technol. **46**, 12069–12078 (2012).
[60]X. Su, S. Zivanovic, and D. H. D'Souza, "Inactivation of human enteric virus surrogates by high-intensity ultrasound," Foodborne Pathog. Dis. **7**, 1055–1061 (2010).
[61]J. Kosel *et al.*, "Efficient inactivation of MS-2 virus in water by hydrodynamic cavitation," Water Res. **124**, 465–471 (2017).
[62]A. Filipić *et al.*, "Hydrodynamic cavitation efficiently inactivates potato virus Y in water," Ultrason. Sonochem. **82**, 105898 (2022).
[63]M. Zupanc *et al.*, "Inactivation of the enveloped virus phi6 with hydrodynamic cavitation," Ultrason. Sonochem. **95**, 106400 (2023).
[64]B. V. Nunes, C. N. da Silva, S. C. Bastos, and V. R. de Souza, "Microbiological inactivation by ultrasound in liquid products," Food Bioprocess Technol. **15**, 2185–2209 (2022).
[65]J. Smelt, "Recent advances in the microbiology of high pressure processing," Trends food Sci. Technol. **9**, 152–158 (1998).
[66]M. Drábková, H. Matthijs, W. Admiraal, and B. Maršálek, "Selective effects of H_2O_2 on cyanobacterial photosynthesis," Photosynthetica **45**, 363–369 (2007).
[67]Y. Kobayashi *et al.*, "Bactericidal effect of hydroxyl radicals generated from a low concentration hydrogen peroxide with ultrasound in endodontic treatment," J. Clin. Biochem. Nutr. **54**, 161–165 (2014).
[68]M. M. Rahman, K. Ninomiya, C. Ogino, and N. Shimizu, "Ultrasound-induced membrane lipid peroxidation and cell damage of Escherichia coli in the presence of non-woven TiO_2 fabrics," Ultrason. Sonochem. **17**, 738–743 (2010).
[69]J. Duan and D. L. Kasper, "Oxidative depolymerization of polysaccharides by reactive oxygen/nitrogen species," Glycobiology **21**, 401–409 (2011).
[70]J. Xing *et al.*, "Increasing vaccine production using pulsed ultrasound waves," PLoS One **12**, e0187048 (2017).
[71]M. Shintani *et al.*, "Effect of ultrasound on herpes simplex virus infection in cell culture," Virol. J. **8**, 446 (2011).
[72]W. D. O'Brien, Jr., "Ultrasound–biophysics mechanisms," Prog. Biophys. Mol. Biol. **93**, 212–255 (2007).
[73]M. Dular *et al.*, "Use of hydrodynamic cavitation in (waste) water treatment," Ultrason. Sonochem. **29**, 577–588 (2016).
[74]T. Wierzbicki, W. Li, Y. Liu, and J. Zhu, "Effect of receptors on the resonant and transient harmonic vibrations of Coronavirus," J. Mech. Phys. Solids **150**, 104369 (2021).

[75]M. Yao and H. Wang, "A potential treatment for COVID-19 based on modal characteristics and dynamic responses analysis of 2019-nCoV," Nonlinear Dyn. **106**, 1425–1432 (2021).
[76]C. Liu and C.-W. Wu, "Invariant in variants," Ultrasonics **124**, 106749 (2022).
[77]H. Yao *et al.*, "Molecular architecture of the SARS-CoV-2 virus," Cell **183**, 730–738 (2020).
[78]H. Kinsloe, E. Ackerman, and J. Reid, "Exposure of microorganisms to measured sound fields," J. Bacteriology **68**, 373–380 (1954).
[79]E. C. Dykeman and O. F. Sankey, "Low frequency mechanical modes of viral capsids: An atomistic approach," Phys. Rev. Let. **100**, 028101 (2008).
[80]A. A. Balandin and V. A. Fonoberov, "Vibrational modes of nano-template viruses," J. Biomed. Nanotechnol. **1**, 90–95 (2005).
[81]E. C. Dykeman and O. F. Sankey, "Atomistic modeling of the low-frequency mechanical modes and Raman spectra of icosahedral virus capsids," Phys. Rev. E **81**, 021918 (2010).
[82]K.-T. Tsen *et al.*, "Raman scattering studies of the low-frequency vibrational modes of bacteriophage M13 in water—Observation of an axial torsion mode," Nanotechnology **17**, 5474 (2006).
[83]M. Babincová, P. Sourivong, and P. Babinec, "Resonant absorption of ultrasound energy as a method of HIV destruction," Med. Hypotheses **55**, 450–451 (2000).
[84]Y. Hu and M. J. Buehler, "Comparative analysis of nanomechanical features of coronavirus spike proteins and correlation with lethality and infection rate," Matter **4**, 265–275 (2021).
[85]Y. Hu and M. J. Buehler, "Nanomechanical analysis of SARS-CoV-2 variants and predictions of infectiousness and lethality," Soft Matter **18**, 5833–5842 (2022).
[86]A. Nonn *et al.*, "Inferring mechanical properties of the SARS-CoV-2 virus particle with nano-indentation tests and numerical simulations," J. Mech. Behavior Biomed. Mater. **148**, 106153 (2023).
[87]N. Maroli, "Riding the wave: Unveiling the conformational waves from RBD of SARS-CoV-2 spike protein to ACE2," J. Phys. Chem. B **127**(40), 8525–8536 (2023).
[88]A. C. Eringen, "On differential equations of nonlocal elasticity and solutions of screw dislocation and surface waves," J. Appl. Phys. **54**, 4703–4710 (1983).
[89]K. Guo and M. J. Buehler, "Rapid prediction of protein natural frequencies using graph neural networks," Digital Discovery **1**, 277–285 (2022).
[90]Y. Hu and M. J. Buehler, "Deep language models for interpretative and predictive materials science," APL Mach. Learn. **1**, 010901 (2023).
[91]A. C. Eringen and J. Wegner, "Nonlocal continuum field theories," Appl. Mech. Rev. **56**, B20–B22 (2003).
[92]S. Dastjerdi *et al.*, "On the deformation and frequency analyses of SARS-CoV-2 at nanoscale," Int. J. Eng. Sci. **170**, 103604 (2022).
[93]P. J. Masters, "The molecular biology of coronaviruses," Adv. Virus Res. **66**, 193–292 (2006).
[94]C. Fei *et al.*, "Ultrahigh frequency (100 MHz–300 MHz) ultrasonic transducers for optical resolution medical imagining," Sci. Rep. **6**, 28360 (2016).
[95]T. A. Nguyen and R. K. Gupta, "A view from nano and space technologies: Can gigahertz waves destroy or spread viruses?," Kenk. Nanotec. Nanosci. **7**, 04–13 (2021).
[96]G. Elert, *The Physics Hypertextbook* (Found July, 1998), Vol. 9.
[97]E. Poque *et al.*, "Effects of radiofrequency field exposure on proteotoxic-induced and heat-induced HSF1 response in live cells using the bioluminescence resonance energy transfer technique," Cell Stress Chaperones **26**, 241–251 (2021).
[98]P. Wust *et al.*, "Non-thermal effects of radiofrequency electromagnetic fields," Sci. Rep. **10**, 13488 (2020).
[99]C. Wang, X. Hu, and Z. Zhang, "Airborne disinfection using microwave-based technology: Energy efficient and distinct inactivation mechanism compared with waterborne disinfection," J. Aerosol Sci. **137**, 105437 (2019).
[100]P. Shaw *et al.*, "Evaluation of non-thermal effect of microwave radiation and its mode of action in bacterial cell inactivation," Sci. Rep. **11**, 14003 (2021).
[101]L. Betti *et al.*, "Nonthermal microwave radiations affect the hypersensitive response of tobacco to tobacco mosaic virus," J. Altern. Complementary Med. **10**, 947–957 (2004).
[102]G. Trebbi *et al.*, "Extremely low frequency weak magnetic fields enhance resistance of NN tobacco plants to tobacco mosaic virus and elicit stress-related biochemical activities," Bioelectromagnetics **28**, 214–223 (2007).
[103]D. A. Enderich *et al.*, "Nonlinear transmission line-driven apparatus for short-pulse microwave exposure of aerosolized pathogens," Rev. Sci. Instrum. **92**, 064712 (2021).
[104]B. W. Hoff *et al.*, "Apparatus for controlled microwave exposure of aerosolized pathogens," Rev. Sci. Instrum. **92**, 014707 (2021).
[105]B. W. Hoff *et al.*, "Observed reductions in the infectivity of bioaerosols containing bovine coronavirus under repetitively pulsed RF exposure," IEEE Trans. Biomed. Eng. **70**, 640–649 (2022).
[106]T. Mohorič and U. Bren, "How does microwave irradiation affect the mechanism of water reorientation?," J. Mol. Liq. **302**, 112522 (2020).
[107]G. Y. Solomentsev, N. J. English, and D. A. Mooney, "Hydrogen bond perturbation in hen egg white lysozyme by external electromagnetic fields: A non-equilibrium molecular dynamics study," J. Chem. Phys. **133**, 235102 (2010).
[108]E. Calabrò and S. Magazù, "Viruses inactivation induced by electromagnetic radiation at resonance frequencies: Possible application on SARS-CoV-2," World **10**, 1–4 (2021).
[109]M. C. Santos, C. L. Morais, K. M. Lima, and F. L. Martin, in *Vibrational Spectroscopy in Protein Research* (Elsevier, 2020), pp. 315–335.
[110]T.-M. Liu *et al.*, "Effects of hydration levels on the bandwidth of microwave resonant absorption induced by confined acoustic vibrations," Appl. Phys. Lett. **95**, 173702 (2009).
[111]M. Rosti, S. Olivieri, M. Cavaiola, A. Seminara, and A. Mazzino, "Fluid dynamics of COVID-19 airborne infection suggests urgent data for a scientific design of social distancing," Sci. Rep. **10**, 22426 (2020).
[112]S. Baliga, S. Muglikar, and R. Kale, "Salivary pH: A diagnostic biomarker," J. Indian Soc. Periodontol. **17**, 461 (2013).
[113]H. Fischer and J. H. Widdicombe, "Mechanisms of acid and base secretion by the airway epithelium," J. Membr. Biol. **211**, 139–150 (2006).
[114]S. Koyama *et al.*, "Effects of long-term exposure to 60 GHz millimeter-wavelength radiation on the genotoxicity and heat shock protein (HSP) expression of cells derived from human eye," Int. J. Environ. Res. Public Health **13**, 802 (2016).
[115]M. K. Kolel-Veetil, A. Kant, V. B. Shenoy, and M. J. Buehler, "SARS-CoV-2 infection—Of music and mechanics of its *Spikes*! A perspective," ACS Nano **16**(5), 6949–6955 (2022).
[116]T. Wierzbicki and Y. Bai, "Finite element modeling of alpha-helices and tropocollagen molecules with reference to the spike of SARS-CoV-2," Biophys. J. **121**, 2353–2370 (2022).
[117]J. Chu, "Ultrasound has potential to damage coronaviruses, study finds," Massachusetts Institute of Technology (2021), see https://news.mit.edu/2021/ultrasound-coronaviruses-damage-0316.
[118]B. Adams, I. Sinayskiy, R. van Grondelle, and F. Petruccione, "Quantum tunnelling in the context of SARS-CoV-2 infection," Sci. Rep. **12**, 16929 (2022).
[119]Y. Li, Y. Qu, F. Xie, and G. Meng, "An arbitrary Lagrangian-Eulerian method for nonlinear structural-acoustic interaction of hyperelastic solid and compressible viscous fluid," J. Comput. Phys. **471**, 111665 (2022).
[120]A. Kumar *et al.*, "Quantum-enabled millimetre wave to optical transduction using neutral atoms," Nature **615**, 614–619 (2023).
[121]P. Sulzer *et al.*, "Cavity-enhanced field-resolved spectroscopy," Nat. Photonics **16**, 692–697 (2022).
[122]"What is the point of a database?," Nat. Struct. Mol. Biol. **9**, 495–495 (2002).
[123]National Institutes of Health, see https://www.insdc.org/ for "International Nucleotide Sequence Database Collaboration."
[124]J. Rufo, P. Zhang, R. Zhong, L. P. Lee, and T. J. Huang, "A sound approach to advancing healthcare systems: The future of biomedical acoustics," Nat. Commun. **13**, 3459 (2022).